

Dye-less color filter fabricated by roll-to-roll imprinting for liquid crystal display applications

Hui-Hsiung Lin^{1,2,*}, Chi-hung Lee², and Mao-Hong Lu¹

¹*Department of Photonics and Institute of Electro-Optical Engineering, National Chiao Tung University, Hsinchu 300, Taiwan, Republic of China*

²*Mechanical and Systems Research Laboratories, Industrial Technology Research Institute, Chutung, Hsinchu 310, Taiwan, Republic of China*

* phranklin@itri.org.tw

Abstract: A diffractive grating is promising for color separation to effectively replace conventional absorptive dye color filter in liquid crystal displays. In this paper, we demonstrated a color separation module consisting of an aspheric-lenticular lens array and a blazed grating to substitute for the dye color filter. Each component was designed to match the recent fabrication ability of our roll-to-roll imprinting. The measurement results of a prototype module showed a gain factor of transmission efficiency three times more than that of conventional color filters.

©2009 Optical Society of America

OCIS codes: (220.1920) Diamond machining; (230.1950) Diffraction gratings ;

References and links

1. T. V. Gunn, and W. Haistead, "Diffractive color separation fabrication," Proc. SPIE **3363**, 198–208 (1998).
2. H. Dammann, "Color separation gratings," Appl. Opt. **17**(15), 2273–2279 (1978).
3. M. W. Farn, M. B. Stern, W. B. Veldkamp, and S. Medeiros, "Color separation by use of binary optics," Opt. Lett. **18**(15), 1214–1216 (1993).
4. R. P. Gale, and G. J. Swanson, "Efficient illumination of color AMLCD projection displays using binary optical phase plates," J. Soc. Inf. Disp. **5**(4), 375–378 (1997).
5. C. Joubert, B. Loiseaux, A. Delboulb , and J. P. Huignad, "Phase volume holographic optical components for high-brightness single-LCD projectors," Appl. Opt. **36**(20), 4761–4771 (1997).
6. Y. Taira, H. Numata, D. Nakano, K. Sueoka, F. Yamada, M. Suzuki, M. Noguchi, R. Singh, and E. G. Colgan, "Color filterless liquid crystal illuminated with LEDs," SID 03 Digest **34**, 1250–1253 (2003).
7. R. Caputo, L. D. Sio, M. J. J. Jak, E. J. Hornix, D. K. G. De Boer, and H. J. Cornelissen, "Short period holographic structures for backlight display applications," Opt. Express **15**(17), 10540–10552 (2007).
8. Y. Taira, D. Nakano, H. Numata, A. Nishikai, S. Ono, F. Yamada, M. Suzuki, M. Noguchi, R. Singh, E. G. Colgan, "Low-power LCD using a novel optical system," SID 02 Digest **33**, 1313–1315 (2002).
9. D. K. G. de Boer, R. Caputo, H. J. Cornelissen, C. M. van Heesch, E. J. Hornix, and M. J. J. Jak, "Diffractive grating structures for colour-separating backlights," Proc. SPIE **6196**, 241 (2006).
10. H. H. Lin, and M. H. Lu, "Design of Hybrid Grating for Color Filter Application in Liquid Crystal Display," Jpn. J. Appl. Phys. **46**(No. 8B), 5414–5418 (2007).
11. Y. Taira, F. Yamada, and A. Nishikai, U.S. Patent 6867828 B2(2005).
12. Y. Taira, F. Yamada, and A. Nishikai, U.S. Patent 6667782 B1(2003).

1. Introduction

Liquid crystal display (LCD) is the most widely used terminal component in computer, communication, and consumer electronics due to its thinner size and lighter. To extend its application, it requires cost effectiveness, low power consumption and high image quality. Conventional color filters used in LCD system consist of dyed material, which generates visible colors by transmitting the desired bandwidth of light and absorbing the undesired spectra. In the case of portable display products such as notebook personal computers, low transmissivity directly impacts the power consumption and corresponding battery life. Besides, conventional color filters using dye-gelatin cannot perform high color purity and high efficiency simultaneously; that is because high color purity depends on high coherence light source, whereas high efficiency requires low-absorption and high-transmittance materials. The

other drawbacks of dyed color filters include the induced the heat from the absorption of light [1] and complex fabrication procedure, in which the selective deposition of tri-colored dyed materials onto individually pixellated areas are made.

Several approaches utilizing hologram elements were proposed to supply higher efficiency, lower absorption and higher color purity. H. Dammann firstly used an interleaved structured grating to separate color [2]. To apply in a LCD projector, this method can combine with a micro-optics (spherical lens, cylindrical lens, etc.) array [3–5]. The grating separates the incident light according to its wavelengths, and the micro-optical array generates focal spots for each separated colors. Different types of gratings were used to separate colors, such as the hybrid diffractive–refractive element [3], the fractional Talbot plane of the grating [4] or the holographic component [5]. However, for a LCD monitor, a short-period diffractive grating is usually necessary as the backlight system consists of a thin light-guide [6–9]. To fabricate the short-period grating on the top of a light-guide requires higher production cost and is not suitable for being fabricated using conventional processes such as roll-to-roll or roll-to-sheet printing.

In this article, we propose a roll-to-roll imprinted optical setup consisting of an aspheric-lenticular-lens array and a blazed grating, which is an advanced design for previous study [10] and termed blazed color separation grating (BCSG). Here, the BCSG replaces the conventional color filter films for a red-green-blue (RGB) light-emitting diode (LED) or a cold cathode fluorescent lamp (CCFL) backlight module in the LCD systems. With the aid of an aspheric-lenticular-lens array, the input light can be incident onto the sub-pixels of LCD with less crosstalk.

2. Design

To use the BCSG as color filter in a LCD with CCFL or RGB LED source, a near collimated backlight module is required, as shown in Fig. 1. The light source with three peaks at red (625 nm), green (525 nm) and blue (465 nm) is used. Conventionally, a backlight module consisting of RGB LEDs provides white source with three-peak spectra. However, for the light source of a grating based module, collimation is essential to perform the color division function. Based on the previous research about collimation backlight [11,12], in this study we dedicate to the BCSG and the aspheric-lenticular-lens array.

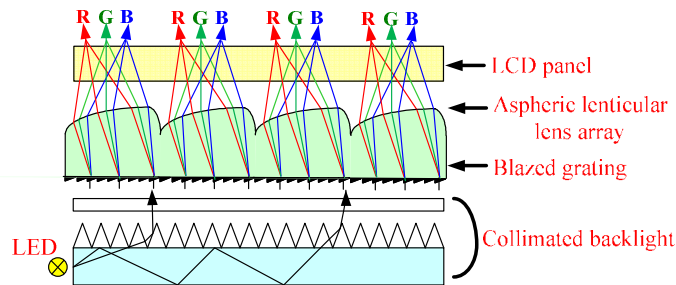


Fig. 1. Schematic representation of a color display with the BCSG. The aspheric-lenticular lens array on top of the grating deflects and converges the incident light. A blazed grating separates the colors in different direction onto the appropriate pixels.

The proposed module consists of a blazed color separation grating (BCSG) and an aspheric-lenticular-lens array. The incident collimated backlight passing through the BCSG is mainly diffracted into a designed order. The angular separation depends on the wavelengths present in its spectrum. The aspheric-lenticular-lens array is then used to converge the deflection beams. In this configuration, the lights of R, G and B emerge at different angles. The blue (B) light and the red (R) light are arrayed to be bilaterally symmetric with respect to the green (G) light, as shown in Fig. 1.

2.1 Design of blazed color separation grating

The grating is used to produce color separation matching the pixel arrangement. A one-dimensional blazed grating is suitable for the geometry, which is designed in such a manner that red, green, and blue bands of a normal incident light are diffracted to a certain order. Diffraction theory including Snell's law is,

$$n \sin \theta = n' \sin \theta' + \frac{m\lambda}{p}. \quad (1)$$

where $\theta' = 0^\circ$ is the incident angle, θ is a diffracted angle, $n' = 1$ is the incident medium refractive index, p is the period, $n = 1.5$ is the refractive index of the diffracted medium and $m = 1$ is the diffraction order. For the practical backlight spectra, the incident white light is not completely collimated. In addition, the spectra distribution of each LED light source is not monochromatic. Therefore, the chromatic aberration shall be considered, as illustrated in Fig. 2. The first-order diffraction angles for different periods at blue (465nm), green (525nm) and red (625nm) are shown in Fig. 3. Considering the process feasibility and the divergence of the emitted light from the backlight module, a grating with pitch = 4 μm is adopted. The first-order diffraction angles are 5.97°, 5.02°, and 4.44° at wavelength 625 nm, 525 nm, and 465 nm, respectively.

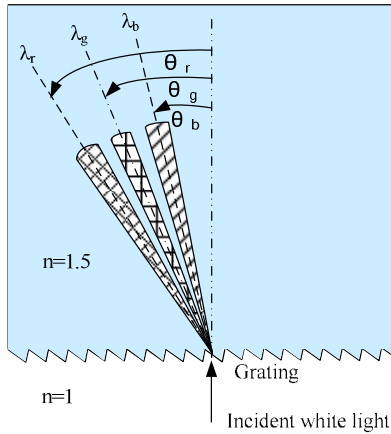


Fig. 2. Configuration of the blazed grating. θ' is designed as 0. θ_r , θ_g and θ_b are the first-order diffraction angles at λ_r , λ_g and λ_b .

In order to have the highest diffraction efficiency, the grating shape in the period has to be optimized. As illustrated in Fig. 4, the period of the grating is denoted as $\Lambda = 4\mu\text{m}$, the maximum depth as h , the blazed angle as α , and the passive angle as β . The incident light of wavelength λ is coming with respect to $\theta' = 0^\circ$ from air into a material with refractive index $n = 1.5$. The d_p is the distance from one-period edge to the center of the groove's peak. The optimized shape is designed to steer the beam to +1st transmitted diffraction order. The ratio of peak position to one period is denoted as cp . The relationship between the grating depth h and the average diffraction efficiency of blue spectra (465nm), green spectra (525nm) and red spectra (625nm) under different cp values is shown in Fig. 5, which indicates that the maximum diffraction efficiency occurs within $cp = 0$ to 0.05 around the grating depth $h = 1\mu\text{m}$. Further simulation shows that if $\alpha = 76^\circ$ and $\beta = 14^\circ$ ($cp = 0.059$ and the grating depth = 0.94 μm), the global maximum diffraction efficiency is ~80%, which is three times more than that of the conventional color filter.

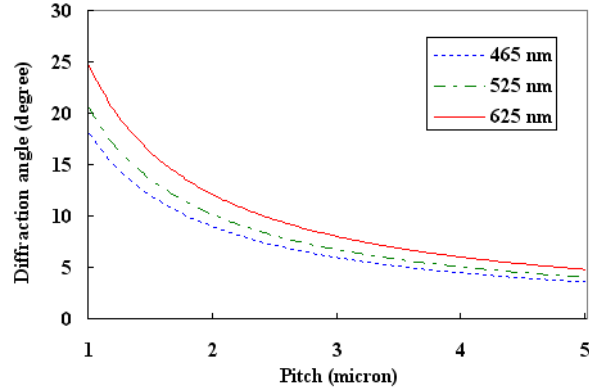


Fig. 3. Variation of the first-order diffraction angle versus the grating period.

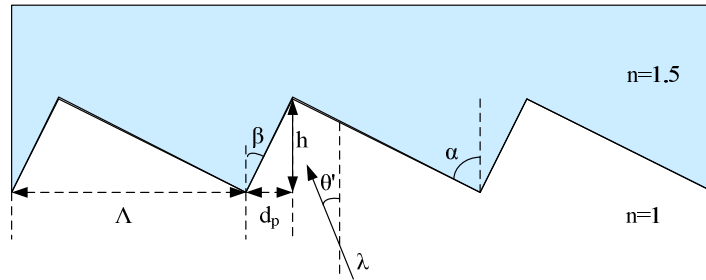


Fig. 4. Geometry of the blazed transmission grating.

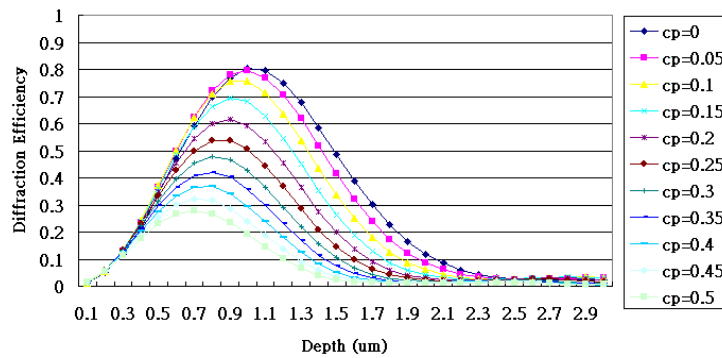


Fig. 5. The relationship between the grating depth h and the average diffraction efficiency of blue spectra (465nm), green spectra (525nm) and red spectra (625nm) under different cp values.

2.2 Design of aspheric-lenticular-lens array and system simulation

The input light should be converged to fit the TFT sub-pixel's size in order to eliminate the crosstalk between the separated colorful beams. Our test sample is a TFT-LCD with the pixel size of $386 \times 420 \mu\text{m}^2$ and every RGB sensing sub-pixel is $128 \times 420 \mu\text{m}^2$. The profile of each pitch ($= 386 \mu\text{m}$) in the aspheric-lenticular-lens array can be derived from the combination of a prism and a spherical lens, which possesses both deflection of -5.02° and convergence, and can be described by the relation,

$$y = \sqrt{4250^2 - (x - 193)^2} - 4245.6 - 0.265 \times (x - 386). \quad (2)$$

where y is the height in micron, 4250 and 4245.6 are related to the curvature radius, 193 and 386 are related to period and x is the position from the edge of each pitch.

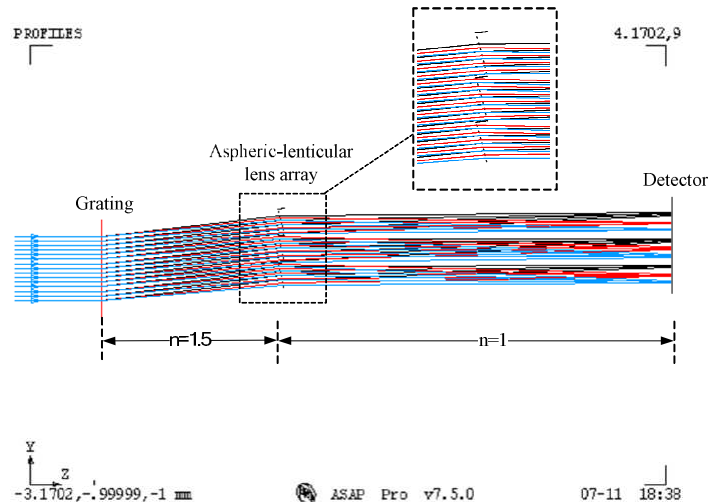


Fig. 6. Illustration of the simulation results. Light from a high collimation backlight module is dispersed by the BCSG, and then deflected and converged by the aspheric-lenticular lens array to generate color separation.

According to Eqs. (1) and (2), a combination of the BCSG with a period of $4\mu\text{m}$ and the aspheric-lens array with a period of $386\mu\text{m}$ was designed to disperse wavelengths. The optical performance has been demonstrated using ASAPTM 7.5 (Advanced Systems Analysis Program) from Breault Research Organization, Inc., which can simultaneously perform ray-tracing geometrical and wave-diffraction physical calculations. Apparently, the split color beams propagate in the nearly normal direction and without crosstalk. A schematic diagram of beam propagation passing through the BCSG and aspheric-lenticular lens array in LCD is shown in Fig. 6.

The process for making the master of the BCSG and the aspheric-lenticular lens array was based on the single-point diamond turning, which used a monocrystal diamond cutting tool with a nanometric edge sharpness to cut the Cu roller. During the machining, the diamond bite was gradually worn within a cutting length, which caused the loss of profile accuracy of the cutting edge. The tolerance about profile of the BCSG was therefore simulated in order to predict the acceptable range of profile deviation. Figure 7a shows the geometry at the start of cutting and Fig. 7b shows the geometry after a cutting distance. A commercial program PCGrate from International Intellectual Group, Inc., was used to solve rigorously the electromagnetic periodic boundary value problems of the grating. The grating's complete efficiency performance was calculated over the entire useable wavelength range under different edge radius of diamond bite, which is denoted as R in Fig. 7b. As shown in Fig. 8, the average diffraction efficiency of replicated gratings with $4\text{-}\mu\text{m}$ pitch is reduced by only 0.5% for $R < 0.2\mu\text{m}$.

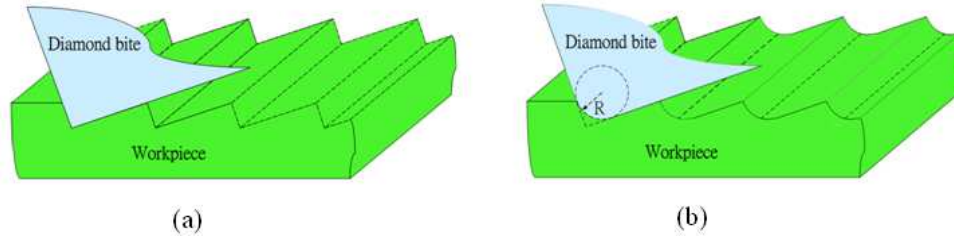


Fig. 7. Variation of edge radius of the diamond bite (a) before and (b) after a cutting distance.

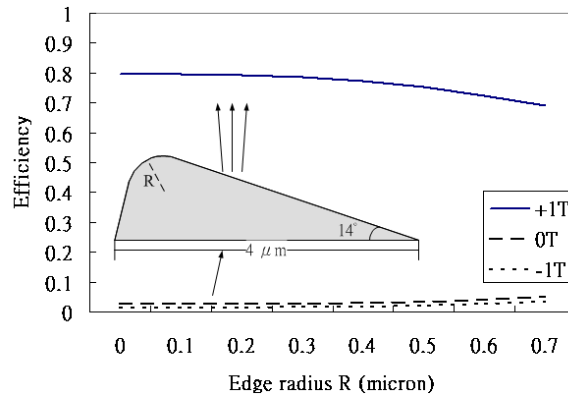


Fig. 8. Calculated diffraction efficiencies of blazed gratings replicated from an imprinting Cu roller, which was cut using various edge radiuses of the diamond bite.

3. Experimental results and discussion

The optical requirements of BCSG in a display configuration are quite challenging, since the diffraction efficiency strongly depends on the value of the period and its profile. Our first aim was to set for a 7-inch LCD display. To make the BCSG and the aspheric-lenticular lens array on a 188 μm thick PET film (T-A4300 by Toray Corp.), a roll-to-roll imprinting process was used. The process can be divided into two steps. First, a mechanically grooved structure was formed on an imprinting Cu roller by using a diamond tool with the designed profile, as shown in Fig. 9(a). Then the UV resin was dispensed on the PET film, imprinted by the roll, hardened by UV curing, and demolded from the roller, as shown in Fig. 9(b).

As one of the most challenging parameters that affected the transforming of the diamond tool's profile (the diamond bite) to the roller, the temperature variation among the diamond tool and the roller surface had to be within $\pm 0.3^\circ\text{C}$, especially in the fabrication of the master for BCSG. Besides, limited to the lifetime of the diamond tool in making BCSG master, the diameter of the roller was as small as possible. In our home-made drum roll lathe, as shown in Fig. 10(a), the diameter of the roller, as shown in Fig. 10(b), was designed to be 200 mm. To make a BCSG-patterned (period = 4 μm) master with a width larger than 100 mm on the surface of our roller, the total cutting length was 15.7 km, which approached the lifetime of a diamond tool.

In the UV curing step, our UV resin (LEN-A by Chishan Corp.) hardened by absorbing energy 500~1000 mJ/cm^2 from UV light. Adequate exposure conditions were indispensable for different micro-structures on the PET film. Since the diffraction efficiency was highly dependent on the grating profile, our major challenge in the curing of BCSG was to achieve high replication rate (>95%). After a series of tests, we found the feed-rate, 3~5 m/min, of feeding UV resin into the roller was the major factor controlling the quality of replication rate. In the curing of the aspheric-lenticular lens array, our major challenge was to completely

demold the pattern after the UV curing, without the need of any master surface treatment. Our tests showed that higher feed-rate, 5~6 m/min, with higher absorbing energy, 900~1100 mJ/cm² from UV light, was the optimal condition to improve antisticking property in demolding. A SEM of BCSG is shown in Fig. 11(a). It has a profile with a period of ~4 μm and a grating depth of 0.90μm. The grating depth is smaller than the designed value, 0.94μm. The difference was mainly caused by the abrasion of the diamond bite during forming the grooved structures on the roller.

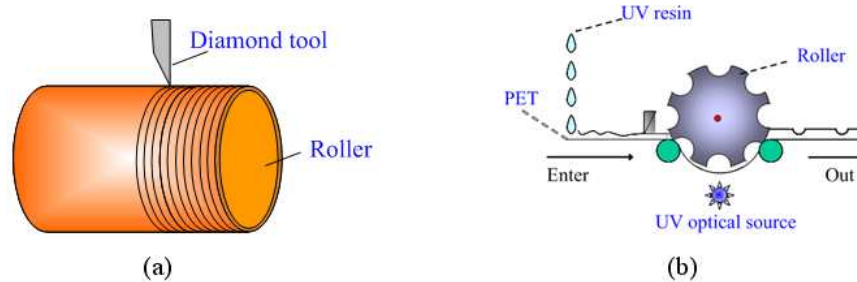


Fig. 9. To make the BCSG and the aspheric-lenticular lens array on a PET film, a mechanically grooved structure was first formed on an imprinting roller by using a diamond tool with the designed profile, as shown in (a). Then the UV resin was dispensed on the PET film, imprinted by the roller, and cured with UV source, as shown in (b).

According to the previous analysis, the loss of diffraction efficiency was smaller than 0.5%. The two blazed angles, α and β , matched our designed values, 76° and 14°. For the BCSG on a PET film, the measured R, G and B transmitting efficiencies were $\eta_{+1, 633\text{nm}} = 65.2\%$, $\eta_{+1, 532\text{nm}} = 76.1\%$ and $\eta_{+1, 473\text{nm}} = 77.3\%$, respectively, which approximated the simulation values after considering the Fresnel loss at the interface between the air and the PET substrate. The procedure to make the aspheric-lenticular lens array on the PET film was the same. A SEM of surface profile of the aspheric-lenticular lens array is shown in Fig. 11(b). It's shape was close to the designed profile with a period of 386 μm and a height of 82.8μm, respectively.



Fig. 10. Pictures of (a) our home-made drum roll lathe and (b) the roller for imprinting the BCSG.

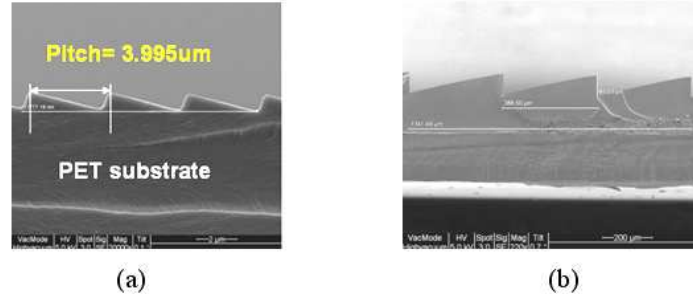


Fig. 11. (a) A SEM of the BCSG. (b) A SEM of the aspheric-lenticular-lens array.

The optical system for testing the module consisting of the BCSG and the aspheric-lenticular lens array is illustrated in Fig. 12. Since the LEDs were not point sources, a collimation setup was arranged for each LED. The iris was used to control the entrance diameter of the incident beam. The aspheric-lenticular lens array was put after the BCSG to produce three convergent separate R/G/B color line pattern.

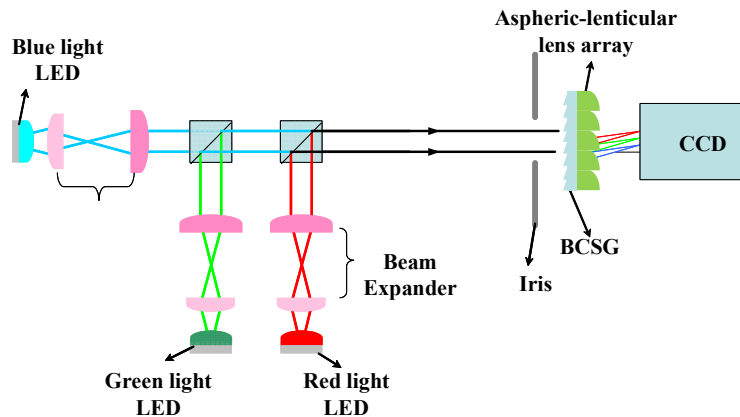


Fig. 12. Optical measurement system for color separation by a module consisting of an aspheric-lenticular lens array and a BCSG.

The system's color characteristic can be defined by the color gamut, which is the range of color a system can reproduce and is commonly expressed as a percentage of NTSC. Although NTSC stands for National Television System Committee, which developed television standards for North America, in this instance, 100% of NTSC refers to the full range of color that can theoretically be displayed. Figure 13 shows the resulting pattern and its xy -color space. The color point for red is shifted to $(x,y) = (0.59,0.29)$ from $(x,y) = (0.69,0.31)$ for the red LED. The color point for green is shifted to $(x,y) = (0.22,0.64)$ from $(x,y) = (0.21,0.75)$ for the green LED. The color point for blue is shifted to $(x,y) = (0.16,0.06)$ from $(x,y) = (0.14,0.03)$ for the red LED. The red line indicates the color gamut (NTSC 73%), and the white dots represent the primary color points of the individual red, green, and blue LEDs (NTSC 117%). The cross section of the resulting line pattern is shown in Fig. 14, which shows the normalized intensity in between the lines does not drop completely to zero. In average, at the position of peak for each line, approximately 9% from the other two colors is visible. The overlap of colors leads to color desaturation, which is caused by several reasons. First, in the measurement setup, each LED had a limit size, which was not a perfect point source and therefore the divergence of the collimation module in the measurement was not completely deleted. Since the first-order diffraction angles of R/G/B are 5.97° , 5.02° , and 4.44° in the design, if the divergence of the collimation module is over $\sim 1^\circ$, overlap of colors will occur. Secondly, the overlap between green and blue is larger than that between green and red. It is

due to an unequal spacing of wavelengths of the light source. The spacing between red and green is 100nm, while the spacing between green and blue is 60nm. Besides, the overlap can be caused by the spherical aberration from the micro-lens array, and by the fact that the spectrum of each LED light source does not simply consist of the monochromatic lines, but a spectrum with a bandwidth of about 40nm. Thirdly, the noise consisted of the diffraction order beams except of the 1st transmitted order one is about 20% of the incident energy, also bleaches the color. Based on these observations, better separation of the colors can be achieved under further optimization of grating and lens profile and of the light source spectrum.

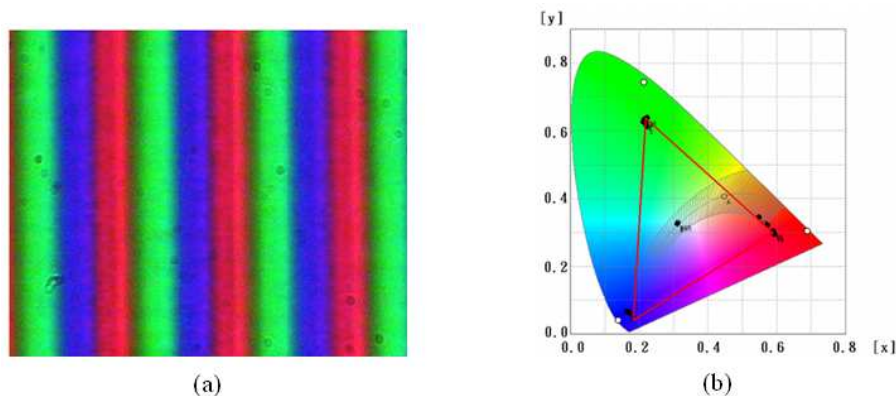


Fig. 13. (a) Color separation patterns of the module consisting of an aspheric-lenticular lens array and a BCSG by making use of RGB LEDs. (b) Color points in CIE xy space, created by sampling the line pattern shown in (a).

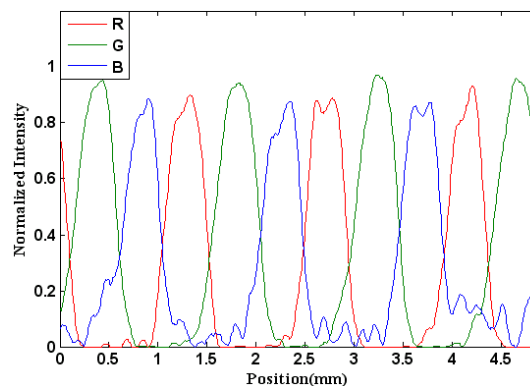


Fig. 14. Normalized intensity distribution of the line pattern generated by the module consisting of the BCSG and the aspheric-lenticular lens array by making use of RGB LEDs.

4. Conclusions

The efficiency of liquid crystal displays can be enhanced by using the diffractive optical element, which separates the incident white light into its spectral components. In this paper, a blazed grating was initially implemented to replace conventional color filters (dye-gelatin and dielectric film, etc.) for a LED backlight module. An aspheric-lenticular lens array was then utilized to converge and deflect the incident beam according to the aperture and spacing of sub-pixels in LC module. The shape of the grating with a period of $4 \mu\text{m}$ was optimized to verify the beam direction and eliminate crosstalk. This module diffracts light into a symmetric RGB pattern. A gain factor of transmission efficiency three times more than that of conventional color filters may be expected. Compared to previous solutions^{6,7}, our system is

based on a collimation backlight module. The advantage of our configuration is that the grating pitch is achievable by using conventional ultra-precision machining, which is suitable for mass-production. For practical use, the divergence of the collimation backlight module shall be reduced to further alleviate the color crosstalk.

Acknowledgements

The authors would gratefully acknowledge Chi-hung Liao for his help with the setup of measurement system and useful discussion. Many thanks to my colleagues at Industrial Technology Research Institute: Chun-Fa Lan and Tsung-Hsin Lin, for the tests of diamond turning on the Cu roller, and Chiun-Lern Fu, for the advice and help in the roll-to-roll imprinting.